American Mineralogist, Volume 70, pages 1027–1035, 1985

Theoretical analysis of chemical and magnetic ordering in the system Fe_2O_3–$FeTiO_3$

BENJAMIN P. BURTON

Alloy Phase Diagrams Data Center
Division 450, Room B150, Building 223
National Bureau of Standards, Gaithersburg, Maryland 20899

A theoretical model of equilibrium phase relations in the system Fe_2O_3–$FeTiO_3$ is presented. This model is based on the single prism approximation in the cluster variation method and includes both chemical and magnetic contributions to the free energy of mixing. The inclusion of a magnetic degree of freedom and magnetic interaction parameters makes it possible to assess the effect of magnetic ordering on the compositions of coexisting titanhematite and hemoilmenite phases, and this effect is shown to be considerable. Two tricritical points are predicted to occur in the Fe_2O_3–$FeTiO_3$ phase diagram: one at which an Fe–Ti order–disorder transition pierces the peak of a two-phase field; and a second at which the two phase field is intersected by an essentially antiferromagnetic transition. Below this latter point, the two-phase field is predicted to bulge out, towards Fe_2O_3, and it is argued that this feature should be useful in geothermometry.

Introduction

In a previous paper (Burton, 1984) this author presented a theoretical model (Model-I) of phase relations in the system hematite–ilmenite (Fe_2O_3–$FeTiO_3$) which required only two energy parameters and achieved rather good agreement with known features of the hematite–ilmenite phase diagram. This model assumed binary mixing of Fe and Ti in corundum and ilmenite structure phases and omitted any treatment of magnetic ordering, an omission which constitutes a serious flaw. The primary purpose of this paper is to present a revised model (Model-II) which includes both chemical and magnetic contributions to the free energy of mixing, and to assess the impact of magnetic ordering on the equilibrium phase relations. It is well known that magnetic interactions can have a significant effect upon equilibrium phase relations (e.g., Meijering, 1963; Miodownik, 1982; Inden, 1982; and Sanchez and Lin, 1984) and in the present case, these effects may have important petrologic implications.

A second purpose of this paper is to elucidate the difference between two types of tricritical points[1] which are predicted to occur in the hematite–ilmenite system:

(1) $\{X_3,T_3\}$-chem, which occurs as a consequence of the anisotropic solution properties of hematite–ilmenite solutions; and

(2) $\{X_3,T_3\}$-mag, which occurs as a consequence of the pseudoternary character of an Fe–Ti solution in which a magnetic degree of freedom exists. Here the term pseudoternary is used because the magnetic degree of freedom enters the calculation as an additional component.

Burton (1984) and Burton and Kikuchi (1984a) described the systems hematite–ilmenite and calcite–dolomite, respectively, as examples of type (1) and the system diopside–jadeite also appears to be of this type (Burton, 1983). An obvious example of type (2) is the system magnetite–ulvospinel which is known to have a miscibility gap at low temperatures (Lindsley, 1981; and Price, 1981) plus a magnetic transition which must intersect the gap. Another example of type (2) may be the alkali feldspars where, instead of a magnetic transition, it is a displacive transition ($C2/m$ monalbite–$C1$ high albite) which intersects the miscibility gap (Thomson and Hovis, 1979). Thus, the results presented below for hematite–ilmenite have implications for many other important rock forming mineral solutions.

Background

The crystal/magnetic structures of antiferromagnetically ordered Fe_2O_3 and chemically ordered $FeTiO_3$ are schematically represented in Figures 1a and 1b, respectively. Both of these structures may be regarded as derivatives of the corundum structure, which can be obtained from either by disordering of Fe↑, Ti, and Fe↓ (Fe↑ = Fe spin-up and Fe↓ = Fe spin-down). Although both Fe_2O_3 and $FeTiO_3$ have additional magnetic transitions, these occur at sufficiently low temperatures that they will not have a significant effect on equilibrium phase relations; therefore, the structures depicted in Figures 1a and 1b may (for the purposes of this work) be treated as ground state configurations of the system without introducing any significant errors.

The experimental and petrographic evidence for chemical ordering and immiscibility in the hematite–ilmentite

[1] Here the phrase *tricritical point* is used, somewhat loosely, to mean the point at which a line of second- or higher-order transitions intersects a miscibility gap or other two-phase field; not in the strict sense of a critical point at which three phases become identical (cf. Scott, 1982 or Knobler and Scott, 1984).

0003–004X/85/0910–1027$02.00

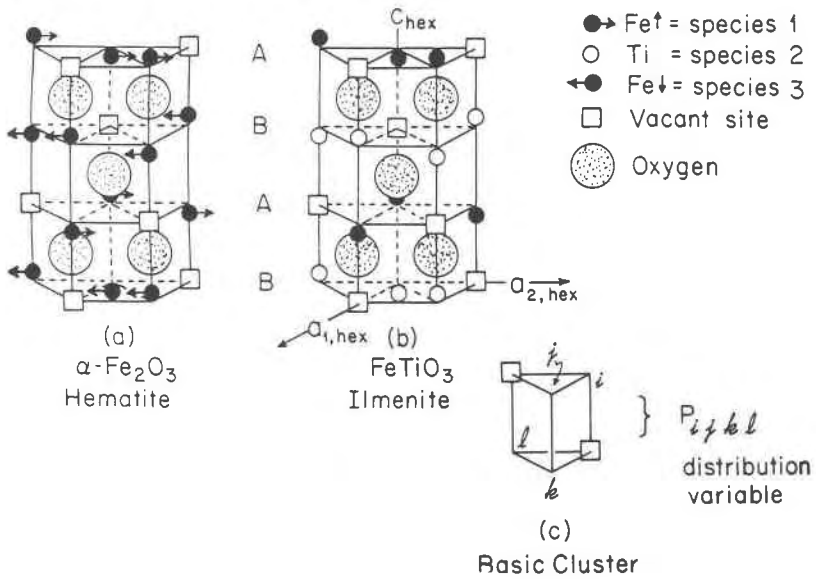

Fig. 1. (a) and (b) Schematic representations of the crystal structures of magnetically ordered hematite and chemically ordered ilmenite, respectively. Arrows on the Fe's in (b) have been omitted to signify disorder of magnetic spins. (c) The single-prism, which is used as the basic cluster for this particular CVM approximation.

system was reviewed by Burton (1984) and is not repeated here. Suffice it to say that the phase diagram is characterized by an order–disorder transition (apparently second-order in character) which intersects a two-phase field at the tricritical point $\{X_3,T_3\}$-chem. The order–disorder transition relates a higher-temperature, more hematite-rich, corundum-structure phase (Hem-ss) to a lower-temperature, more ilmenite-rich, ilmenite-structure phase (Ilm-ss); Hem-ss + Ilm-ss is the stable assemblage in the two-phase region (Model-I faithfully reproduces this phase topology). In addition to these features, there is also a line of antiferromagnetic–paramagnetic transition (also apparently second order in character) which follows an approximately linear trend of $T_N(X) = 950–1790X$ [$T_N(X)$ is the Néel temperature, X is the cationic fraction of Ti (equal to mole fraction of Ti_2O_3), and temperature is in Kelvins; Ishikawa and Akimoto, 1957]. Below this line, Hem-ss is essentially antiferromagnetic (with a weak parasitic moment, cf. Lindsley, 1976) and is referred to as AF-ss. The intersection of this line with the two-phase field implies the presence of a second tricritical point ($\{X_3,T_3\}$-mag) and at temperatures below T_3-mag AF-ss + Ilm-ss must be the stable two-phase assemblage (Model-II is necessary to account for these features).

Models

Both Models-I and -II are based on the single prism approximation (SPA, Burton and Kikuchi, 1984b; Burton, 1984) in the cluster variation method (CVM; Kikuchi, 1951). The CVM defines a hierarchical set of approximate solutions to the Ising model problem in which the configurational free energy is written as a function of the internal energies and probabilities of occurence (concentration varibles) for each possible configuration of atoms on some small basic cluster or clusters of sites. When individual sites are the largest clusters considered, the Bragg-Williams approximation results as a degenerate case; and when pairs of sites are the largest clusters, the Bethe quasi-chemical approximation results. Two significant advantages are associated with the use of higher order (larger cluster) approximations:

1. Symmetry constraints, consistent with space group symmetry, are imposed on the calculated values of concentration variables and these constraints are sometimes essential for obtaining correct transition behavior and therefore correct phase topology. For example, the tetrahedron approximation of the CVM correctly predicts that the order–disorder transition in CuAu is first order in character (Kikuchi, 1977) but the Bragg–Williams and Bethe approximations predict a second order transition.

2. Higher order approximations include detailed information about short range order and therefore yield substantially improved approximations of the configurational entropy and associated thermodynamic functions. For example, when the Néel temperature of Fe_2O_3 is calculated from the magnetic coupling constants of Samuelsen and Shirane (1970) the Bragg–Williams approximation yields a value that is 1.36 times the observed T_N wheres $T_{N\text{-SPA}} = 1.21T_{N\text{-obs}}$ (Burton and Kikuchi, 1984b); an improvement which is a direct result of including short range order in the SPA.

In the present case, the Bragg–Williams approximation is sufficient to obtain appropriate transition behavior and phase topology, so the benefits of resorting to the SPA are

primarily quantitative in nature. Specifically, the SPA yields improved estimates of the thermodynamic functions associated with the stabilization of ilmenite, relative to mechanical mixing of $(Fe_2O_3 + Ti_2O_3)/2$ (see below); and as implied by the example given above, requires less drastic modification to obtain agreement between $T_{\text{N-calc}}$ and $T_{\text{N-obs}}$.

In the SPA the basic cluster consists of four occupied sites and two vacant sites (Fig. 1c) and it is assumed that all mixing of components occurs on the sites designated as occupied. Model-I assumed mixing of only two components (Fe and Ti) while Model-II considers three (Fe↑, Ti, and Fe↓). This increase in the number of components increases the number of variables to be solved for (from 16 to 81) but does not otherwise alter the SPA-CVM equations. Thus equation (6) in Burton (1984) may be used as is for Model-II. This equation is given below and readers interested in its derivation should consult the earlier paper and Burton and Kikuchi (1984b).

$$\ln X(4)_{ijkl} = \beta\lambda + A_{ij} + B_{kl} + \beta\{(1/6)[\mu_i + \mu_j + \mu_k + \mu_l] - \varepsilon_{ijkl}\} + \ln \frac{[X(3,1)_{ijk}X(3,2)_{jkl}X(2,4)_{il}]^{1/2}[X(2,2)_{ij}X(2,3)_{kl}]^{1/4}}{[X(1,1)_iX(1,1)_jX(1,2)_kX(1,2)_l]^{1/4}[X(2,1)_{jk}]^{1/6}} \quad (1)$$

Where: (1) Variables of the form $X(r,t)_{ijk\ldots}$ are the concentration variables for r-body clusters of t-type in configuration $ijk\ldots$. For example: $X(4)_{ijkl}$ is the concentration of 4-body clusters (single prisms) in configuration $ijkl$; $X(3,2)_{jkl}$ is the concentration of 3-body clusters of type-2 in configuration jkl; and $X(1,1)_i$ is the concentration of 1-body clusters of type-1 (equal to the concentration of species-1 on type-1 sites)[2]; (2) $i,j,k,l = 1$, 2, and 3; for components Fe↑, Ti, and Fe↓ respectively, e.g., $X(4)_{1322}$ is the concentration of single prisms in configuration {Fe↑Fe↓TiTi}; (3) $\beta = (kT)^{-1} = [(\text{Boltzmans constant})(\text{absolute temperature})]^{-1}$; (4) λ, A_{ij}, and B_{kl} are Lagrange multipliers which impose constraints of normalization and space group symmetry on the solution; (5) μ_i is the chemical and/or magnetic potential of component i; (6) ε_{ijkl} is the total energy of a single prism in configuration $ijkl$, which is assumed to be a sum of chemical [W(r)'s] and magnetic [J(r)'s] pairwise interaction parameters for r'th neighbor pairs.

Equations (1) can be solved by the natural iteration method (as in Burton and Kikuchi, 1984b) at fixed values of T and μ; where μ is defined as the chemical potential of Fe↑ or Fe↓ in the absence of an applied magnetic field:

$$\mu \equiv \mu_1 = \mu_3 = -\mu_2 \quad (2)$$

Only one chemical potential variable is independent because the constraints of normalization and zero applied field require that:

$$0 = \mu_{Fe\uparrow} + \mu_{Ti} + \mu_{Fe\downarrow} = \mu_1 + \mu_2 + \mu_3 \quad (3a)$$

and

$$\mu_{Fe\uparrow} = \mu_{Fe\downarrow} = -\mu_{Ti} = \mu_1 = \mu_3 = -\mu_2 \quad (3b)$$

respectively. In the presence of an applied magnetic field it would be necessary to fix T and two of the μ_i's in order to solve for the $X(4)_{ijkl}$'s, and in this case

$$\mu_{Fe\uparrow} = \mu + \mu^m \quad (4a)$$

$$\mu_{Fe\downarrow} = \mu - \mu^m \quad (4b)$$

$$\mu_{Ti} = -\mu \quad (4c)$$

where μ^m is the magnetic potential in the ↑-direction.

Equilibrium compositions of coexisting phases were determined by the same method that was used in Burton (1984) but the calculation of second-order transition points was not. Instead, the approach of Sanchez and de Fontaine (1978) was used because it is much easier and more systemmatic. This method is based on differentiation of the free energy with respect to an independent set of correlation functions to obtain the Hessian matrix (matrix of second derivatives with respect to independent variables). The application of this method to two component systems is described by Sanchez and de Fontaine (1978); the extension to three component systems is given by Kikuchi et al. (1980); and the generalization to n-component systems is presented in Sanchez et al. (1984).

Total energy

The essential difference between Models-I and -II is in the term ε_{ijkl} in equation (1). Model-I included only the chemical contribution which is given by

$$\varepsilon_{ijkl} = \varepsilon_{\text{chem}} = \frac{\delta_{jk}}{6} W(1) + \frac{\delta_{ij} + \delta_{kl}}{4} W(2) \quad (5)$$

where $\delta_{ij} \equiv ||i - 2| - |j - 2||$

$$= \begin{cases} 1 & \text{for Fe}\uparrow - \text{Ti or Fe}\downarrow - \text{Ti nn-pairs} \\ 0 & \text{otherwise} \end{cases} \quad (6)$$

and the factors of 1/6 and 1/4 correct for the number of prisms which "share" an interaction [eg. 6 prisms share $W(1)$]. Note that the indices $ijkl$ on ε_{chem} have been dropped for ease of writing, but are nonetheless understood to be present, the same applies to ε_{mag} below.

The parameters $W(1)$ and $W(2)$ are the excess energies for the formation of Fe–Ti near-neighbor cation–cation pairs (nn-pairs) along the hexagonal c-axis (c-hex) and within the hexagonal basal plane, respectively. The W(r)'s are defined so that $W(1) < 0$, indicating that the formation of Fe–Ti nn-pairs along c-hex lowers the free energy; and $W(2) > 0$, indicating that the formation of Fe–Ti nn-pairs within basal planes, increase it [relative to mechanical mixing of $(1 - X)Fe_2O_3 + XTi_2O_3$].

In Model-II a magnetic contribution is added to equation (5) so that

$$\varepsilon_{ijkl} = \varepsilon_{chem} + \varepsilon_{mag} \quad (7)$$

[2] The $X(r,t)_{ijk\ldots}$ notation for concentration variables differs from the notation used in Burton (1984) and Burton and Kikuchi (1984b) but since it is more informative and less arbitrary the change seems justified. Concentration variables in equation (1) above are equivalent to variables in equation (6) of Burton (1984b) which have identical indices.

where

$$\varepsilon_{mag} = \frac{\delta'_{jk}}{6} J(1) + \frac{\delta'_{ij} + \delta'_{kl}}{4} J(2) + \frac{\delta'_{il}}{2} J(3) + \frac{\delta'_{ik} + \delta'_{jl}}{2} J(4) \quad (8)$$

$$\text{and } \delta'_{ij} \equiv -(i-2)(j-2) = \begin{bmatrix} 1 & \text{for Fe}\uparrow - \text{Fe}\downarrow \\ 0 & \text{for Fe}\uparrow - \text{Ti, Fe}\downarrow - \text{Ti} \\ -1 & \text{for Fe}\uparrow - \text{Fe}\uparrow, \text{Fe}\downarrow - \text{Fe}\downarrow \end{bmatrix} \quad (9)$$

The $J(r)$'s (magnetic coupling constants) in equation (8) have been determined for stoichiometric Fe_2O_3 by Samuelsen and Shirane (1970) and these $J(r)$'s [$J^0(r)$'s below] are taken as a starting point for formulating ε_{mag} in Model-II. Two modifications of the $J^0(r)$'s are made in order to improve agreement between the calculated and experimentally determined curves for $T_N(X)$:

(1) A scale factor (A) is applied to all $J^0(r)$'s so that calculated and observed values of $T_N(X=0)$, stoichiometric Fe_2O_3, will agree.

(2) A many body parameter (B) is used to make the strength of magnetic coupling [$|J(r)$'s$|$], in a given cluster configuration, a function of the Ti-concentration in that configuration [$x\{ijkl\}$].

$$x\{ijkl\} = \frac{4 - |i-2| - |j-2| - |k-2| l-2|}{4} \quad (10)$$

Thus

$$J(r) + A[1 - Bx\{ijkl\}]S_z^2 J^0(r) \quad (11)$$

where S_z is the saturation moment of Fe^{3+} in stoichiometric Fe_2O_3. Clearly the variables S_z and A are not independent and the value for A given below assumes that $S_z = 5/2$. Parameter B is used to give $T_N(X)$ a more negative slope than would occur by simple magnetic dilution of Fe_2O_3 as is observed experimentally.

The nature of magnetic coupling in Hem-ss and AF-ss is obviously complicated by the coupled substitution of $Fe^{2+} + Ti^{4+}$ for $2Fe^{3+}$ which implies that Fe^{3+}–Fe^{2+} coupling (and perhaps more complicated charge transfer phenomena; Warner et al., 1972) would have to be considered in an ab initio calculation. Also, the presence of Fe in distinct valence states would require that additional components be included in the expression for the configurational entropy. It should be noted, however, that these complications are most important for compositions near $X = 0.25$ (halfway between Fe_2O_3 and $FeTiO_3$); and, therefore, the approximations in Model-II are not expected to have a particularly adverse effect upon the estimated stabilization of $FeTiO_3$, or the phase topology in the neighborhood of $\{X_3, T_3\}$-mag. This is so because complications associated with Fe's in different valence states do not apply for stoichiometric $FeTiO_3$ (where all iron is Fe^{2+}, e.g., Lindsley, 1976); and because $\{X_3, T_3\}$-mag occurs at a rather Fe-rich composition [$X_3 \approx 0.12$], where a model based on perturbed Fe_2O_3 coupling should be reasonably good.

Results and discussion

Figures 2, 3 and 4 present the results of Model-II calculations that were performed with the following parameters: $W(1) = -22.86$ kJ/mole, $W(1) = -W(2)/3$ (as in Model-I); $J^0(1) \ldots J^0(4)$ (the "probable values" of Samuelsen and Shirane, 1970; as in Burton and Kikuchi, 1984b) $A = 0.803$ (with $S_z = 5/2$) and $B = 2.0$. Note that the ratio $W(1)/W(2) = -3$ is the same in Models-I and -II.

Stabilization of $FeTiO_3$

Figure 2 illustrates the roles of oxidation-reduction and cation ordering in the stabilization of $FeTiO_3$, relative to $(Fe_2O_3 + Ti_2O_3)/2$. The ΔH-values plotted in Figure 2 are calculated from the 298 K and one bar values in the tables of Robie et. al. (1979).

$$\Delta H(\text{Ilm}) = \Delta H(FeTiO_3) - [\Delta H(Fe_2O_3) + \Delta H(Ti_2O_3)]/2$$
$$= \Delta H(\text{Redox}) + \Delta H(\text{Ord}). \quad (12)$$

Note that with the above choice of parameters

$$\Delta H(\text{Ord})_{SPA} = W(1) \approx -23 \text{ kJ/mole};^3 \quad (13)$$

because $B = 2.0$, implies that $\varepsilon_{mag} = 0$ for all clusters which contain two or more atoms of titanium (equations 7–11).

The formation of $FeO + TiO_2$ from $(Fe_2O_3 + Ti_2O_3)/2$ involves the same redox reaction that is required to form randomly disordered $FeTiO_3$ ($Fe^{3+} + Ti^{3+} \rightarrow Fe^{2+} + Ti^{4+}$). This reaction does not, however, involve the added stabilization due to cation ordering which occurs in ilmenite. Because FeO and TiO_2 retain the six-fold coordination of metal ions (by oxide ions) that is present in the corundum and ilmenite structures, it is expected that

$$\Delta H(\text{Redox}) = \Delta H(FeO + TiO_2) \quad (14a)$$

and therefore

$$\Delta H(\text{Ord}) \approx \Delta H(\text{Ilm}) - \Delta H(FeO + TiO_2) \approx -20 \text{ kJ/mole} \quad (14b)$$

The value of $\Delta H(FeO + TiO_2)$ varies considerably between 298 K and 1600 K (Robie et. al., 1979), however the value of ΔH(Ord) (equation 14b) remains remarkably constant at about -20 kJ/mole from 298 K to 1200 K. Above 1200 K, ΔH(Ord) increases slightly to -17 kJ/mole at 1500 K then decreases again to -20 kJ/mole at 1600 K (ilmenite melts at 1640 K). Therefore, it seems reasonable to assume that -20 kJ/mole is a good approximation for ΔH(Ord), and given the apparent temperature independence of ΔH(Ord) this value is probably more realistic than the estimate of -18 kJ/mole which was used in Burton (1984, Table 2).

Also shown in Figure 2, is the result one obtains when the Bragg–Williams approximation is used and $T_C(FeTiO_3)$ is held constant, $\Delta H(\text{Ord})_{BW} = -14$ kJ/mole. The improved agreement between $\Delta H(\text{Ord})_{SPA}$ and ΔH(Ord) of equation 14b, relative to $\Delta H(\text{Ord})_{BW}$, is a direct consequence of including structural information and short range order in the SPA, and thereby obtaining an improved approximation of the configurational entropy. Note that if

[3] It should be noted that the value reported for ΔH(Ord) of Model-I (Burton, 1984) was erroneously given as -8 kJ/mole but is actually $\Delta H(\text{Ord}) \approx -23$ kJ/mole, an error which resulted from careless dimensional analysis.

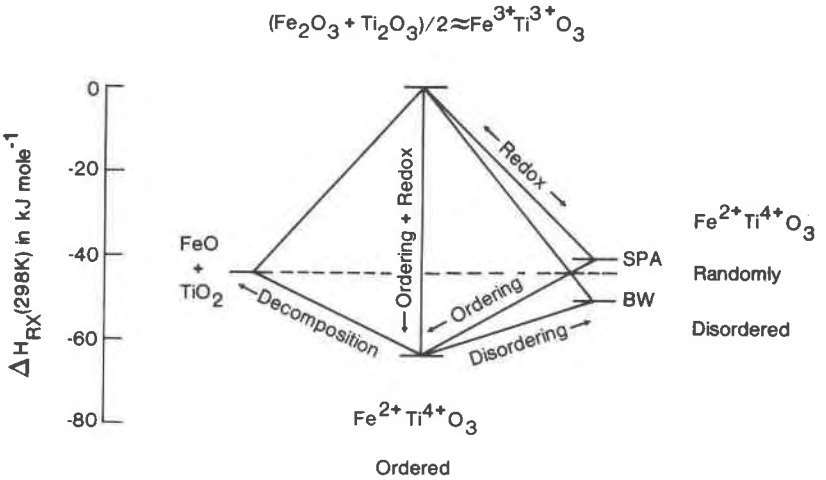

Fig. 2. Born–Haber cycles indicating the contributions to the stabilization of $FeTiO_3$, from oxidation–reduction and cation ordering. Results of Model-II (SPA) are compared to results the Bragg–Williams approximation (BW) and to the formation of FeO + TiO_2, which involves approximately the same redox reaction. All experimental values for enthalpies of formation (at 298 K and one bar) are from Robie et al. (1979).

ΔH(Ord) is fixed at the value of -20 kJ/mole then $T_{C-BW} = 2132$°C and $T_{C-SPA} = 1199$°C.

The very large discrepancy between $\Delta H(\text{Ord})_{BW}$ and $\Delta H(\text{Ord})_{SPA}$ [or equivalently, between T_{C-BW} and T_{C-SPA}, when ΔH(Ord) is fixed] reflects the strong proclivity for short range order which is predicted by the SPA, a result which is related to the phenomenon of critical dimensionality. It is well known that one dimensional systems can not transform to a state with long range order, although they can develop very strong short range order (cf. Ziman, 1972). Similarly, when a system is constructed of weakly connected one dimensional systems, the weak connections control the transition temperature, because thermal disordering of these connectors reduces the effective dimensionality of the system below the critical limit. Such a system will have a depressed transition temperature (relative to a system with equally strong interactions in two or three dimensions) and very strong short range order above T_C. The ilmenite structure approximates such a system in the sense that interactions along c-hex may be regarded as isolated one dimensional pair systems which are connected by weaker two dimensional interactions within the basal plane. The SPA includes this structural information and therefore predicts very strong short range order above $T_C(FeTiO_3)$ or equivalently, a more negative ΔH(Ord) for a fixed value of T_C. Note, however, that the discrepancy between $T_N(Fe_2O_3)_{BW}$ and $T_N(Fe_2O_3)_{SPA}$ is much smaller than the discrepancy with respect to ΔH(Ord) because magnetic coupling is strong in all three dimensions.

Chemical potential vs. reduced temperature

Figure 3 is a selected portion of the chemical potential vs. reduced temperature diagram, where T_C is the estimated critical temperature for stoichiometric $FeTiO_3$. On this diagram, two phase fields (in composition vs. temperature space) are reduced to lines that indicate the value of chemical potential at which two phases coexist. Two such fields are indicated by the solid and dash–dot lines, Hem-ss + Ilm-ss and AF-ss + Ilm-ss respectively (labeled as $R\bar{3}c$

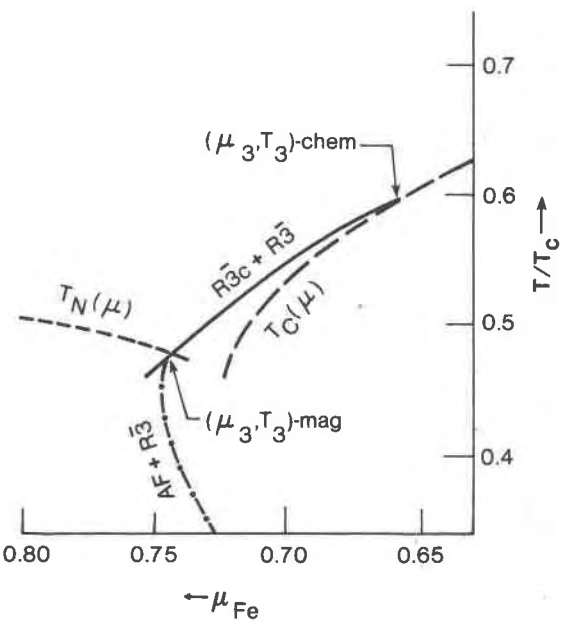

Fig. 3. A portion of the chemical potential of iron vs. reduced temperature diagram ($\mu \equiv \mu_{Fe\uparrow} = \mu_{Fe\downarrow} = -\mu_{Ti}$ vs. T/T_C), calculated with Model-II. The solid and dash-dot lines indicate values of μ at which two phases coexist; and the dashed lines labeled $T_C(\mu)$ and $T_N(\mu)$ indicate second order instabilities with respect to chemical and magnetic ordering respectively. Note that the $T_C(\mu)$ line meets the solid $R\bar{3}c + R\bar{3}$ line at the bifurcation point $\{\mu_3, T_3\}$-chem but the $T_N(\mu)$ line cuts right across it as $\{\mu_3, T_3\}$-mag.

+ $R\bar{3}$ and AF + $R\bar{3}$ respectively). The dashed lines labeled $T_C(\mu)$ and $T_N(\mu)$ indicate second-order instabilities with respect to chemical and antiferromagnetic ordering respectively. Note that the curves for $T_C(\mu)$ and Hem-ss + Ilm-ss bifurcate at $\{\mu_3,T_c\}$-chem; as do the curves for Hem-ss + Ilm-ss and AF-ss + Ilm-ss at $\{\mu_3,T_3\}$-mag. The curve for $T_N(\mu)$ however, extends across the two-phase line and does not merge into it.

Composition vs. temperature

Figure 4 is the theoretical phase diagram in which the effects of magnetic interactions are immediately apparent; particularly with respect to the "symmetries" of the two-phase fields. Above T_3-mag the Hem-ss + Ilm-ss region ($R\bar{3}c$ + $R\bar{3}$) is said to be "asymmetric" in the sense that more ilmenite will dissolve in Hem-ss than hematite in coexisting Ilm-ss. Below T_3-mag the composition of AF-ss, coexisting with Ilm-ss changes very rapidly and with decreasing temperature, the AF-ss + Ilm-ss (AF + $R\bar{3}$) region becomes approximately symmetric. This bulge in the AF-ss + Ilm-ss field is perhaps the most important prediction of Model-II; the implication is that a narrow temperature range T_3-mag > $T \gtrsim$ [T_3-mag–50°C] separates symmetric and asymmetric two-phase regions, a result which may be useful in geothermometry.

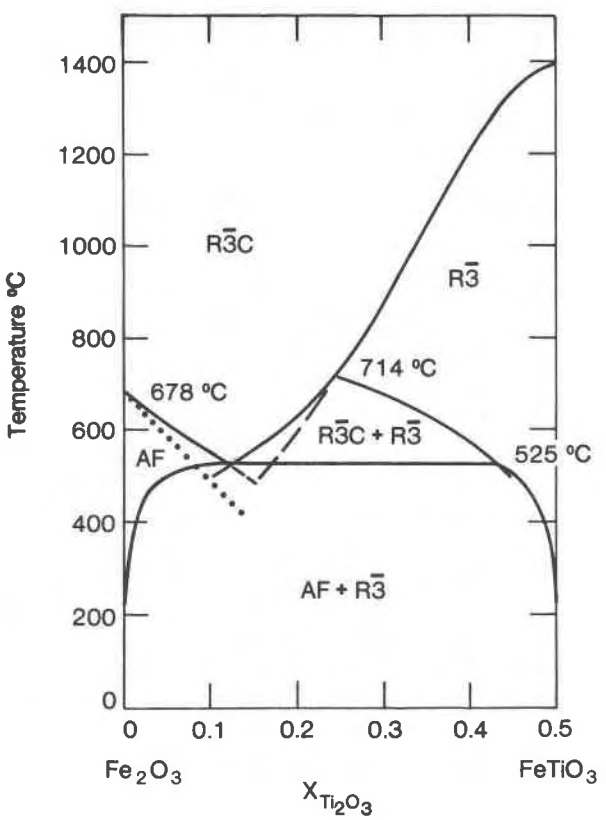

Fig. 4. Theoretical temperature-composition diagram for the system Fe_2O_3–$FeTiO_3$; $R\bar{3}c$ indicates the disordered corundum structure phase; $R\bar{3}$ indicates the chemically ordered ilmenite structure phase; and AF indicates the antiferromagnetic phase. Note that the calculated slope of the $T_N(X)$-curve is somewhat less negative than the experimental curve (dotted).

Note that the calculated slope of $T_N(X)$ is somewhat less negative than the experimental value determined by Ishikawa and Akimoto (1957; dotted line, Fig. 4). It is possible to improve the agreement between calculated and experimental curves, but to do so requires additional perturbation parameters in the expression for ε_{mag}; for example one could make $\varepsilon_{mag} = 0$ in any cluster which contained one or more Ti's. It should be noted, however, that Model-II estimates $T_N(X)$ for an equilibrium distribution of cations rather than a quenched high-temperature distribution as was examined by Ishikawa and Akimoto (1957) so that the two curves are not exactly comparable. Clustering of Fe's and Ti's near $\{X_3,T_3\}$-mag is expected to slightly increase $T_N(X)$ and, therefore, the correct equilibrium curve may lie slightly above the experimental one.

Tricritical points

To illustrate the role of anisotropic solution properties in generating $\{X_3,T_3\}$-chem it is helpful to plot the chemical contribution to the excess enthalpy of mixing as a function of composition [assuming that $\Delta H(\text{xs}) = \Delta E(\text{xs})$]. Evaluating ΔH(xs) in the two extreme cases of random disorder and perfect order generates the two curves plotted (schematically[4]) in Figure 5. For these extreme cases, the results are identical to a Bragg–Williams approximation in which both first- and second-neighbor interactions are included. For pedagogical purposes, this model is most convenient and is therefore developed below. First neighbor pairs occur along the hexagonal c-axis (**c**-type pairs) and are associated with the parameter $W(1) < 0$; second neighbor pairs occur within the basal planes (**a**-type pairs) and are associated with $W(2) > 0$. The chemical contribution to excess enthalpy of mixing is given by

$$\Delta H(\text{xs}) = \Delta H(\mathbf{c}) + \Delta H(\mathbf{a}) \tag{15a}$$

$$\Delta H(\mathbf{c}) = W(1)Z(\mathbf{c})[X - X^2(1 - S^2)] \tag{15b}$$

$$\Delta H(\mathbf{a}) = W(2)Z(\mathbf{a})[X - X^2(1 + S^2)] \tag{15c}$$

where: S is the long range order parameter; $Z(\mathbf{c}) = 1$ is the coordination number of **c**-type pairs; $Z(\mathbf{a}) = 3$ is the coordination number for **a**-type pairs; and $0 < X < 0.5$ (to consider $0.5 < X < 1.0$, X is redefined as cationic fraction of Fe rather than Ti).

Equation (15b) is the usual Bragg–Williams term for the excess enthalpy associated with ordering and is derived by expressing the site occupancies as functions of X and S then assuming that the probability of forming a **c**-type pair is equal to the product of appropriate site occupancies.

$$X(2,1)_{12} + X(2,1)_{21} = X(1,1)_1X(1,2)_2 + X(1,1)_2X(2,1)_1 \tag{16}$$

[4] Figure 5 was actually generated with $W(1) < -3W(2)$ to emphasize positive deviations from ideality, in ΔH^{xs}. With $W(1) = -3W(2)$ as in Model-II, $\Delta H^{xs}(S = 0) = 0$ and $\Delta H^{xs}(S = 1) \leq 0$ for all values of X.

Equation (15c) is derived in the same way but in this case the probability of formation of an **a**-type pair is considered

$$X(2,2)_{12} + X(2,3)_{12} = X(1,1)_1X(1,1)_2 + X(1,2)_1X(1,2)_2. \quad (17)$$

Note that $X(2,2)_{12} = X(2,2)_{21}$ and $X(2,3)_{12} = X(2,3)_{21}$. The right-hand side of equation (15c) has the same (composition)(order) dependence $(-X^2S^2)$ as the "enthalpy of disordering" term invoked by Navrotsky and Loucks [1977, equation 7; $\Delta H(\text{dis}) = WX^2(1 - S^2)$]; and, with respect to pure composition dependence, the Navrotsky and Loucks formulation simply replaces $X(1 - X)$ with X^2. Since equation (15c) arises naturally from the consideration of **a**-type pairs, whereas the Navrotsky and Loucks formulation is ad hoc, equation (15c) should be preferred for problems of this kind.

From Figure 5 it is clear why both ordering and immiscibility characterize the phase relations of this system; in the random case (S = 0) $\Delta H(\text{xs})$ has the form which is typical for a system with a miscibility gap, [$\Delta H(\text{xs}) > 0$ and parabolic, with a maximum at $X = 0.5$]; in the perfectly ordered (S = 1) case however, $\Delta H(\text{xs})$ is greater than zero for small and large values of X but has a negative minimum at $X = 0.5$. This result obtains because the ordered layer structure (Fig. 1b) is stabilized by **c**-type pairs but avoids the formation of destabilizing **a**-type pairs (an avoidance which can be complete only at $X = 0.5$). Thus, the anisotropy of $\Delta H(\text{xs})$ favors the formation of an ordered structure for $0.25 \lesssim X \lesssim 0.75$ but also favors phase separation for $0 < X \lesssim 0.25$ and $0.75 \lesssim X < 1.0$; and because **a**-type pairs must be created when $X \neq 0.5$ (even for S = 1) chemically ordered single-phase material will always be metastable for X less than some critical value [$X_3 \lesssim 0.25$].

Because $\Delta H(\mathbf{c})$ and $\Delta H(\mathbf{a})$ vary sympathetically and continuously with bulk composition, a continuous change from ordering alone to ordering plus phase separation occurs. This, together with the second-order character of the chemical order–disorder transition, explains why (in Fig. 3) the $T_C(\mu)$ and Hem-ss + Ilm-ss curves bifurcate at $\{\mu_3,T_3\}$-chem. In contrast, however, the $T_N(\mu)$ curve cuts right across the two-phase equilibrium curve, because the Néel transition depends upon the independent magnetic degree of freedom which enters the calculation as an additional component. Finally, bifurcation of the curves Hem-ss + Ilm-ss and Af-ss + Ilm-ss, at $\{\mu_3,T_3\}$-mag, occurs because the Néel transition is second-order in character and, therefore, AF-ss, in equilibrium with Ilm-ss, transforms continously into Hem-ss, in equilibrium with Ilm-ss.

Petrologic implications

Intergrowths of Hem-ss + Ilm-ss are fairly common in metamorphic rocks (e.g., Rumble, 1976 and Richardson and Essene, 1985) and also occur in some plutonic rocks such as the anorthosite complex at Allard Lake (Charmichael, 1961). Typically, these intergrowths are asymmetrically exsolved and in the cases considered by Rumble (1976), the higher-temperature Hem-ss + Ilm-ss assemblage ("garnet and staurolite metamorphic mineral zone") is replaced, at lower temperatures, by one of the three-phase assemblages; Hem-ss (AF-ss?) + magnetite + rutile; or Ilm-ss + magnetite + rutile, ("chlorite and biotite zone"). Carmichael (1961) reported the coexistence $X = 0.035$ and $X = 0.44$ material, possibly AF-ss + Ilm-ss, which would be roughly consistent with a 500°C isotherm in Figure 4. However, the compositions determined by Carmichael were based primarily

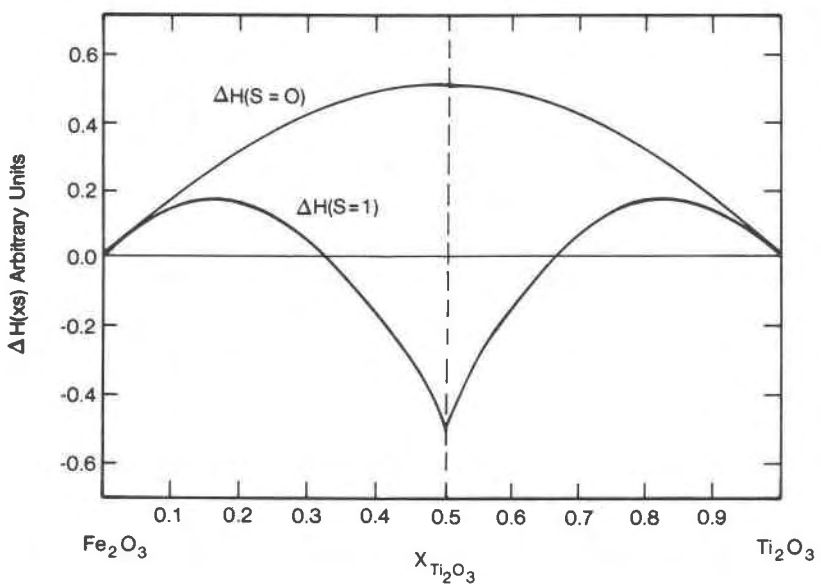

Fig. 5. The chemical contribution to the excess enthalpy of mixing, plotted schematically for the extreme cases of random disorder (upper curve) and perfect long range order (lower curve).

on the results of thermal demagnetization studies and Hargraves (pers. comm.) reports that microprobe analyses of the titanhematite lamellae in Allard Lake ores indicate $X \approx 0.125$, inconsistent with the magnetic property data.

To this author's knowledge, no convincing examples of symmetrically exsolved intergrowths have been reported in metamorphic or plutonic rocks and there are several plausible explanations for this situation:

(1) The two-phase assemblage may become unstable or metastable relative to a three phase assemblage;

(2) AF-ss may occur only as very small late-stage lamellae, too small to be correctly analyzed with an electron microprobe;

(3) The blocking temperature for exsolution may occur above T_3-mag;

(4) Energy barriers due to coherency may prevent formation of the equilibrium assemblage;

It is not clear which of the above explanations (or some other explanation) might be correct, but in any case, T_3-mag at least marks a minimum temperature for strongly asymmetric Hem-ss + Ilm-ss assemblages. Also, it is interesting to note that T_3-mag occurs at a temperature which is reasonable for the transition from Rumble's "chlorite and biotite zone" to his "garnet and staurolite zone", and may therefore, coincide with the transition from two-phase to three-phase stability. Surely, the most favorable conditions for the formation of stable AF-ss + Ilm-ss include a very slow cooling rate and a highly oxidizing $f(O_2)$ and in rocks formed under such conditions, the occurence of this assemblage should be regarded as a distinct possibility.

Conclusions

It is predicted that two tricritical points occur in the hematite–ilmenite phase diagram: one related to anisotropy of solution properties $\{X_3,T_3\}$-chem; and a second related to the interplay of magnetic ordering and chemical phase separation $\{X_3,T_3\}$-mag. Above the latter point, an asymmetric Hem-ss + Ilm-ss field occurs and below it, an approximately symmetric AF-ss + Ilm-ss field is predicted. Although convincing examples of the AF-ss + Ilm-ss assemblage have not been reported (to this author's knowledge), this assemblage may well occur in intergrowths formed under conditions of very slow cooling and rather oxidizing $f(O_2)$; and it is hoped that this article will stimulate efforts to find it. Even if AF-ss + Ilm-ss never occurs in nature, T_3-mag may still be regarded as a minimum temperature for strongly asymmetric Hem-ss + Ilm-ss coexistence and therefore, marks an approximate isotherm which should be useful to petrologists.

Acknowledgments

The author wishes to thank R. L. Scott for comments which provided the motivation for this work; and also R. B. Hargraves and C. A. Lawson for helpful comments concerning magnetic properties. This work was completed while the author was a National Research Council Associate in the ceramic processing group at the National Bureau of Standards.

References

Burton, B. P. (1983) CVM analysis of the system $CaMgSi_2O_6$–$NaAlSi_2O_6$. EOS, 64, No. 45, 869.

Burton, B. P. (1984) Thermodynamic analysis of the system Fe_2O_3–$FeTiO_3$. Physics and Chemistry of Minerals, 11, 132–139.

Burton, B. P. and Kikuchi, R. (1984a) Thermodynamic analysis of the system $CaCO_3$–$MgCO_3$ in the tetrahedron approximation of the cluster variation method. American Mineralogist, 69, 165–175.

Burton, B. P. and Kikuchi, R. (1984b) The antiferromagnetic-paramagnetic transition in α-Fe_2O_3 in the single prism approximation of the cluster variation method. Physics and Chemistry of Minerals, 11, 125–131.

Carmichael, C. M. (1961) The magnetic properties of ilmenite-hematite crystals. Proceedings of the Royal Society, A, 263, 508–530.

Inden, G. (1982) The effect of continuous transformations on phase diagrams. Bulletin of Alloy Phase Diagrams, 2, 412–422.

Ishikawa, Y. and Akimoto, S. (1957) Magnetic properties of the $FeTiO_3$–Fe_2O_3 solid solution series. Journal of the Physical Society of Japan, 12, 1083–1098.

Kikuchi, R. (1977) The cluster variation method. Journal De Physique, Colloque C7, supp. 12, Tome 38, 307–313.

Kikuchi, R. (1951) A theory of cooperative phenomena. The Physical Review, 81, 988–1003.

Kikuchi, R. Sanchez, J. M., deFontaine, D. and Hisao Yamauchi (1980) Theoretical calculation of the Cu–Ag–Au coherent phase diagram. Acta Metallurgica, 28, 651–662.

Knobler, C. M. and Scott, R. L. (1984) Multicritical points in fluid mixtures: experimental studies. In C. Dom and J. L. Lebowitz, Ed., Phase Transitions and Critical Phenomena, 9, 163–231, Academic Press, New York.

Lindsley, D. H. (1976) The crystal chemistry and structure of oxide minerals as exemplified by the Fe–Ti oxides; Experimental studies of oxide minerals. In D. R. Rumble, Ed., Oxide Minerals. Reviews in Mineralogy, 3, Mineralogical Society of America, p. L1–L88.

Lindsley, D. H. (1981) Some experiments pertaining to the magnetite–ulvospinel miscibility gap. American Mineralogist, 66, 759–762.

Meijering, J. L. (1963) Miscibility gaps in ferromagnetic alloy systems. Phillips Research Reports, 13, 318–330.

Miodownik, A. P. (1982) The effect of magnetic transformations on phase diagrams. Bulletin of Alloy Phase Diagrams, 2, 406–412.

Navrotsky, A. and Loucks, D. (1977) Calculation of subsolidus phase relations in carbonates and pyroxenes. Physics and Chemistry of Minerals, 1, 109–127.

Price, G. D. (1981) Subsolidus phase relations in the titanomagnetite solid solution series. American Mineralogist, 66, 751–758.

Richardson, S. V. and Essene, E. J. (1985) Ilmenite and hematite from the Chapata copper deposit, Brazil and their constraints on the ilmenite–hematite solvus. Contributions to Mineralogy and Petrology, in press.

Robie, R. A., Hemingway, B. S. and Fisher, J. R. (1979) Thermodynamic properties of minerals and related substances at 298.15 K and 1 Bar (10^5 Pascals) pressure and at higher temperatures. Geological Survey Bulletin 1452. United States Government Printing Office, Washington, D.C.

Rumble, D. R. (1976) Oxide Minerals. Reviews in Mineralogy, 3, Mineralogical Society of America, p. R1–R24.

Samuelsen, E. J. and Shirane, G. (1970) Inelastic neutron scatter-

ing investigation of spin waves and magnetic interactions in α-Fe_2O_3. Physics Status Solidi, 42, 241–256.

Sanchez, J. M., Ducastelle, F. and Gratias, D. (1984) Generalized cluster description of multicomponent systems. Physica, 128A, 334–350.

Sanchez, J. M. and de Fontaine, D. (1978) The fcc Ising model in the cluster variation method approximation. Physical Review, B17, 2926–2936.

Sanchez, J. M. and de Fontaine, D. (1980) Ordering in fcc lattices with first- and second-neighbor interactions. The Physical Review B21, 216–228.

Sanchez, J. M. and Lin, C. H. (1984) Modeling of magnetic and chemical ordering in binary alloys. The Physical Review, B30, #3, 1448–1453.

Scott, R. L. (1982) Multicritical phenomena in fluid mixtures. In J. V. Sengers, Ed., Proceedings of the Eighth Symposium on Thermophysical Properties: Thermophysical properties of fluids, Volume 1, p. 397–404. The American Society of Mechanical Engineers.

Thompson, J. B. and Hovis, G. L. (1979) Structural–thermodynamic relations of the alkali feldspars. In Transactions of the American Crystallographic Association; Proceedings of the Symposium on Chemistry and Physics of Minerals. American Crystallographic Association.

Warner, B. N., Shire, P. N., Allen, J. A. and Terry, C. (1972) A study of the hematite–ilmenite series by the Mössbauer effect. Journal of Geomagnetism and Geoelectricity, 24, 353–367.

Ziman, J. M. (1972) Principles of the Theory of Solids, second edition, p. 353–366. Cambridge University Press.

Manuscript received, October 10, 1984;
accepted for publication, May 6, 1985.